

Fluid Structure Interaction (FSI) Simulation Of the human eye under the air puff tonometry using Computational Fluid Dynamics (CFD)

O. Maklad^{*,1}, V. Theofilis¹ and A. Elsheikh^{1,2}
Corresponding author: O.Maklad@liverpool.ac.uk

¹ School of Engineering, University of Liverpool, Liverpool, UK.

² NIHR Biomedical Research Centre for Ophthalmology, Moorfields Eye Hospital NHS
Foundation Trust and UCL Institute of Ophthalmology, UK.

Abstract: The air puff test is a non-contact method used in different areas to investigate the material behaviour or the biomechanical properties of biological tissues such as skin, cornea, and soft tissue tumours and also to study fruit firmness or meat tenderness. For the human eye, having a valid and fully coupled numerical simulation of the air puff test is very helpful and can greatly benefit to reduce a lot of time and cost of experimental testing. The gap in research in this area is considering the fluid structure interaction effect between the cornea, the air puff and the eye internal fluid. The simulation of the air puff test on the human eye is a Multi-physics problem which means; coupling between different numerical models and solvers with different governing equations and exchanging the data between them during the solution. A Computational Fluid Dynamics (CFD) model has been generated for an impinging air jet of maximum velocity of 168 m/s over a time span of 30ms and a coupling between the CFD model and the Finite Element (FE) model of the human eye has been successfully achieved for accurate simulation of the Fluid Structure Interaction (FSI) effect on the human eye cornea deformation.

Keywords: Human eye, Non-Contact Tonometry, Ocular biomechanics, Glaucoma, Intra-Ocular Pressure (IOP), Computational Fluid Dynamics (CFD), Finite Element Analysis (FEA), Fluid Structure Interaction (FSI), Impinging jets, Aeroelasticity.

1 Introduction

The human eye contains a viscoelastic fluid called vitreous humour and has a pressure called Intraocular pressure (IOP), which gives the eye its spherical shape. This pressure is crucial and is very important to understand everything related to it. There are a lot of ocular diseases connected directly or indirectly to IOP, if it's deviated from its normal values. Some of these diseases are Glaucoma, Ocular Hypertension and Retinal Detachment. Glaucoma is one of the ocular diseases which develops when the eye internal fluid cannot drain properly and the intraocular pressure builds up. This can result in damage to the optic nerve and the nerve fibres from the retina and early diagnosis is very important as any damage to the eyes cannot be reversed. Accurate measurement of the intraocular pressure (IOP) is essential in management of Glaucoma and diagnosis of other diseases. The two most common types of Glaucoma are Open Angle Glaucoma (OAG) and Angle Closure Glaucoma (ACG). In 2010, more than 44.7 million patients are diseased with OAG and 15.7 million patients with ACG. The numbers are expected to increase in 2020 to 58.6 million OAG patients and 21 million ACG patients [1].

The gold standard of IOP measurement and the most widely accepted method is the Goldmann applanation tonometry (GAT), developed in the 1950s [2]. It is based on the force measurement required to flatten

or applanate the cornea surface to estimate the IOP value. However, the GAT measurement is affected by the biomechanics of the cornea such as corneal thickness (CCT), material properties and curvature (R).

The contact tonometry involves direct contact between the device and the cornea. However, the non-contact tonometry uses a rapid air pulse to applanate or flatten the cornea and the IOP is measured by detecting the force of the air jet at the moment of applanation. CorVis-ST and Ocular Response Analyser (ORA) are two devices use this concept in the IOP measurement. The aim of this study is to improve the accuracy of the IOP measurements by considering the fluid structure interaction effect between the cornea, the air puff and the eye internal fluid through a parametric study of numerical models and their comparisons with the clinical data.

Numerical simulation, if it's Computational Fluid Dynamics (CFD) or Finite Element Analysis (FEA), is a very important tool in biomechanics scientific research as it can give better understanding for unseen behaviour or save time and effort of experimental testing for running parametric studies or extracting material properties. For the air puff test simulation, numerical methods are the core of the work and understanding the different governing equations and different solvers is essential. The air puff test simulation consists of three pillars:

- Finite element and material model for the eye based on accurate topography and geometry.
- CFD turbulence modelling of the air puff impinging at the cornea.
- The FSI coupling between the two models.

1.1 Impinging jet basic theory

The basic theory of the CFD impinging air puff is the round jet diffusion and impingement theory. The impinging jets have different variety of important applications such as cooling and drying, they are also representative models for the jets in vertical take-off and landing aircrafts and rockets or in the simulation of the atmospheric microbursts. The flow characteristics of impinging jets depend on different parameters, such as jet orifice diameter, nozzle to impingement surface distance, jet confinement, radial distance from stagnation point, angle of impingement, surface curvature & roughness, nozzle exit geometry and turbulence intensity [3], [4], [5]. By studying the air puff and its flow characteristics, it has been found that it's a turbulent jet with Reynolds number (23702.26) which means that we need to simulate highly disturbed flow with turbulent eddies and vorticities. The jet split into 3 regions; the "free" jet region, the impingement or stagnation region, and the wall-jet region, see Figure 1.

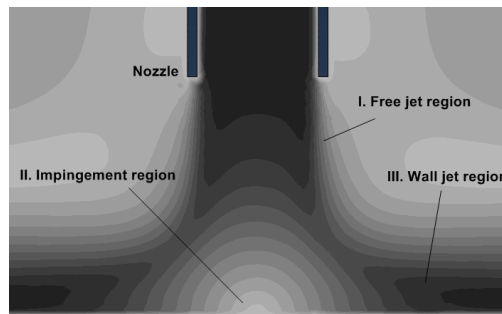


Figure 1: Impinging jet different regions.

Reynolds Averaged Navier-Stokes equations (RANS) are the governing equations for the CFD model, simply they represent the mass and the momentum conservation in differential form in the three dimensions. These equations will simulate the flow, but we still need an appropriate turbulence model to resolve and capture the large and small eddies. Abaqus-CFD has 3 different models, "Spalart-Allmaras" as a one equation RANS model, "RNG and Realizable K- ϵ models" and "K- ω model" as a two equations RANS model.

1.2 Aeroelasticity

Aeroelasticity deals with the combined features of fluid dynamics and solid mechanics. There are many applications based on this part of science such as aircraft’s wing design, turbo-machinery, bridges and skyscrapers design, electric transmission lines, artificial heart valves, respiratory mechanics and is considered as the foundation of the modern biomechanics. In most of the aeroelasticity applications, it’s normally assumed that the external loading acting on a structure is, in general, independent of the deformation of that structure and this was the assumption made in the literature when simulating the air puff test, but actually the deformations of the cornea are in an order of magnitude which can’t be ignored compared to the eye and the cornea size and it will have effect on the applied aerodynamic force by the air jet. The key reference dimensionless number in specifying the kind of the FSI problem is the Reduced Velocity $U_R = \frac{T_{Solid}}{T_{Fluid}}$ which is the ratio between the two time scales of the coupled models. In the air puff test U_R is in order of magnitude from (0 to 10) which is close to the displacement number of the structure model (0.054). This range of the reduced velocity is the range of the general aeroelasticity problem which require full coupling and consideration of both time scales during the solution and solving the two models simultaneously at the same time. The quasi-static and pseudo-static aeroelasticity approaches will have a great impact on the accuracy of the solution as there is no model dominant over the other.

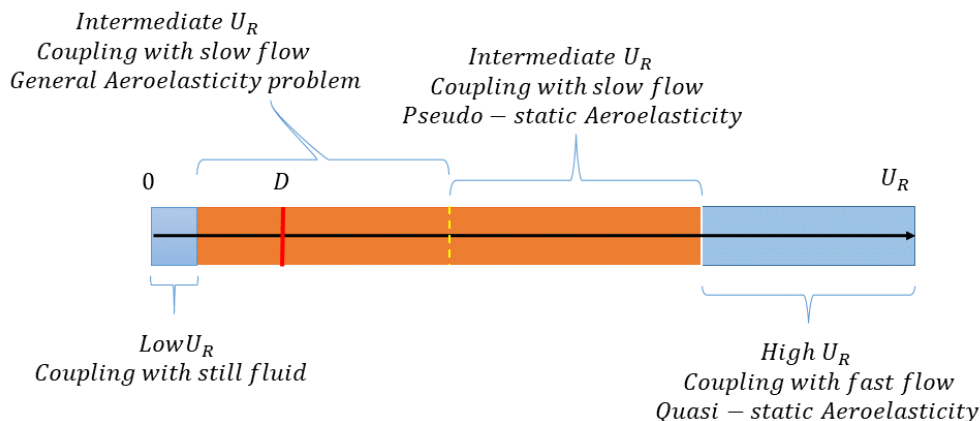


Figure 2: The classification of aeroelasticity problems based on the reduced velocity U_R .

2 Numerical simulation methodology

The three main parts of the air puff test simulation are the eye model, the CFD model of the air jet and the FSI coupling between them. The process starts by modelling the CFD model of the air jet first and making sure that it’s working separately without any coupling or interfaces and considering the cornea as no-slip wall boundary condition. Then, the finite element model of the eye is coupled with the CFD turbulent model of the air puff exchanging the characteristic variables between them at every time step of the job as shown in figure 3.

2.1 CFD setup

The air domain geometry, figure 4 has been generated by Matlab code to project the coordinates of the cornea and three rings from the sclera into layers above the eye model till we reach a distance of 11 mm which is the typical distance for the test on real patients. Then, the fluid material properties are defined as

air in terms of density and kinematic viscosity. The boundary conditions are applied inlet, outlet and no-slip wall BCs. After making sure that the CFD model is working on its own, the cornea and sclera surfaces are changed into Fluid Structure Interaction interface and the eye input file is modified to add the lines of the co-simulation region and the FSI interface. Then, a co-execution job has to be generated and the two models have to run at the same time exchanging information between them.

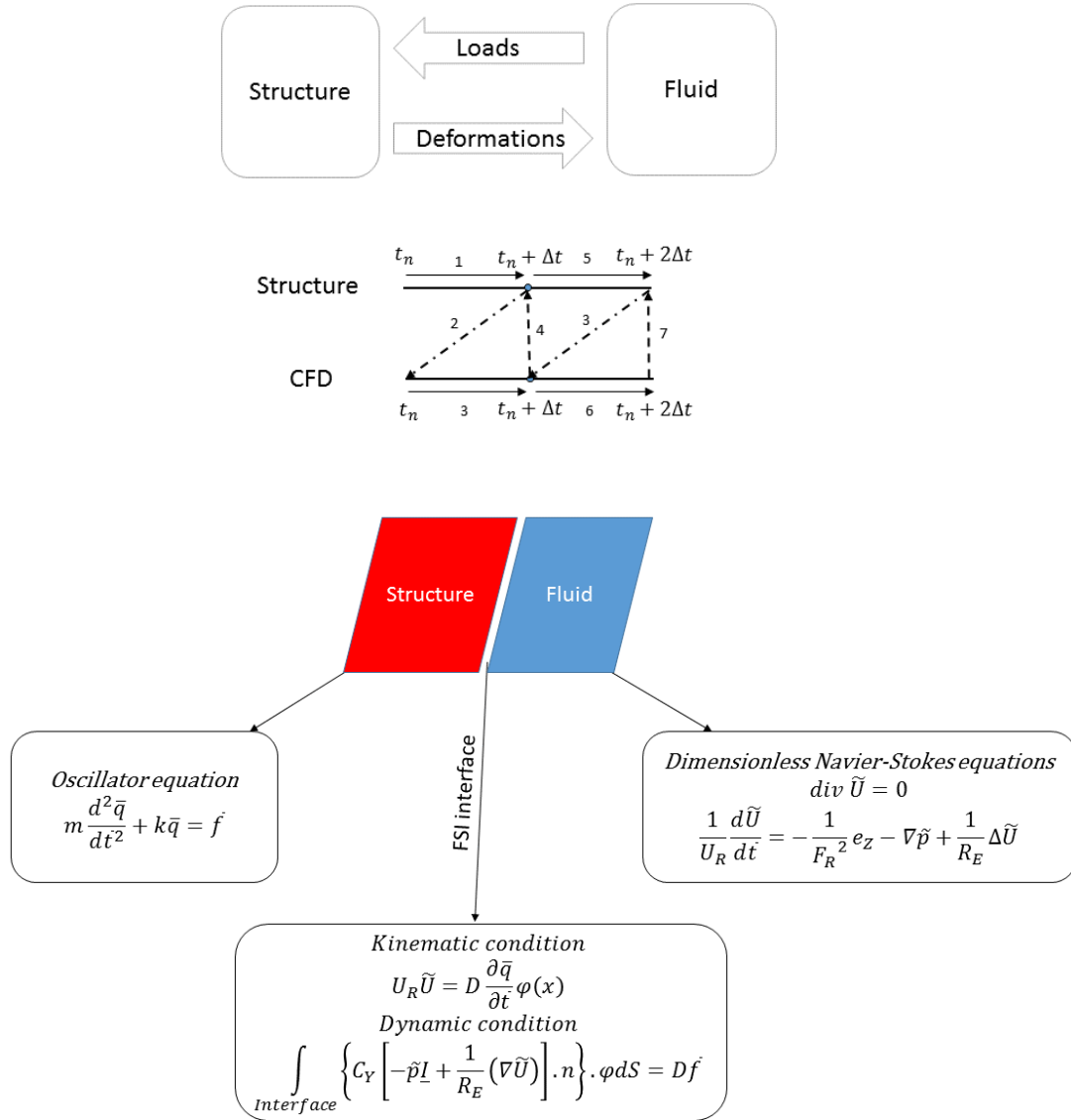


Figure 3: The Idea of Fluid Structure Interaction and coupled dimensionless equations.

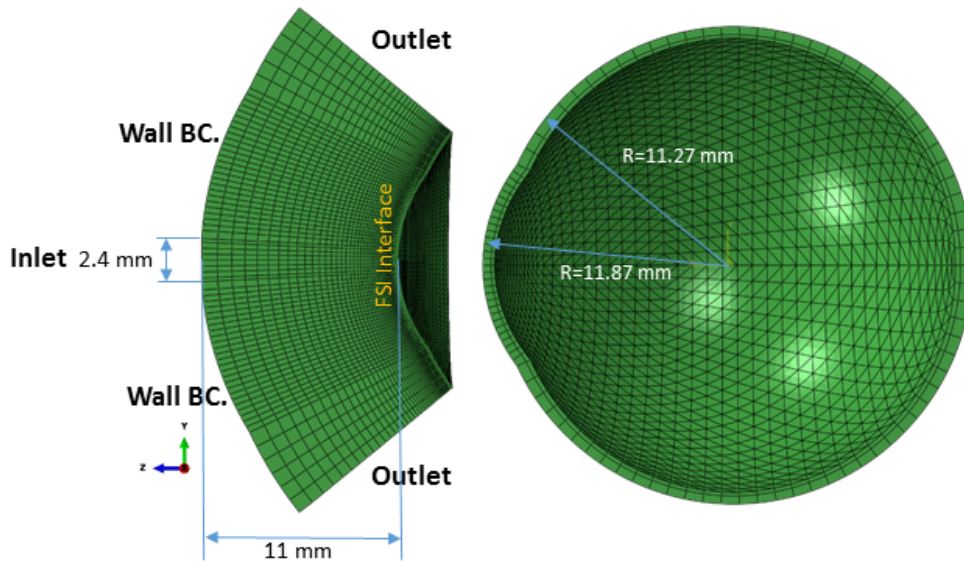


Figure 4: The CFD and Eye models mesh and geometry definition.

2.2 CSD setup

The finite element model of the eye is generated by orphan mesh technique through node, element and input files with Abaqus special syntax. The Eye model has to be fixed in space from the equatorial nodes, the internal loading of the IOP has to be applied first on a separate step to inflate the eye from the stress free geometry and lastly the most important part is the material properties definition for the different section of the eye, based on previous published research done in the Biomechanics group.

2.3 FSI setup

After making sure that the CFD model is working on its own, the cornea and part from the sclera surfaces are changed into Fluid Structure Interaction interface and the eye input file is modified to add the lines of the co-simulation region and the FSI interface. Then, a co-execution job has to be generated and the two models have to run at the same time exchanging the characteristic variables, forces and deformations.

3 Results

In this section the validation of Abaqus/CFD as turbulent flow solver will be presented first and then the FSI model of the air puff test and comparison of the corneal deformation with a clinical case will be shown.

3.1 Abaqus/CFD validation

To validate the CFD code available in Abaqus an impinging air jet on a fixed wall of bulk velocity of 9.6 m/s for Tummers experiment [6] and the numerically reproduced flow field on Abaqus CFD using Spallart Allmaras turbulence model are shown in figure 5. It shows good agreement with the flow field of the Laser Doppler Anemometer (LDA) experimental mean flow field. The mean axial and radial velocities at different axial traverses normal to the impingement surface are shown in table 1 and 2

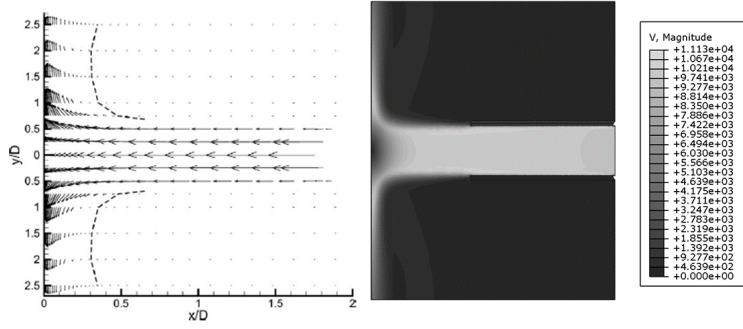


Figure 5: Laser Doppler Anemometer (LDA) mean flow field for Tummers experiment and the reproduced numerically flow field on Abaqus-CFD [6].

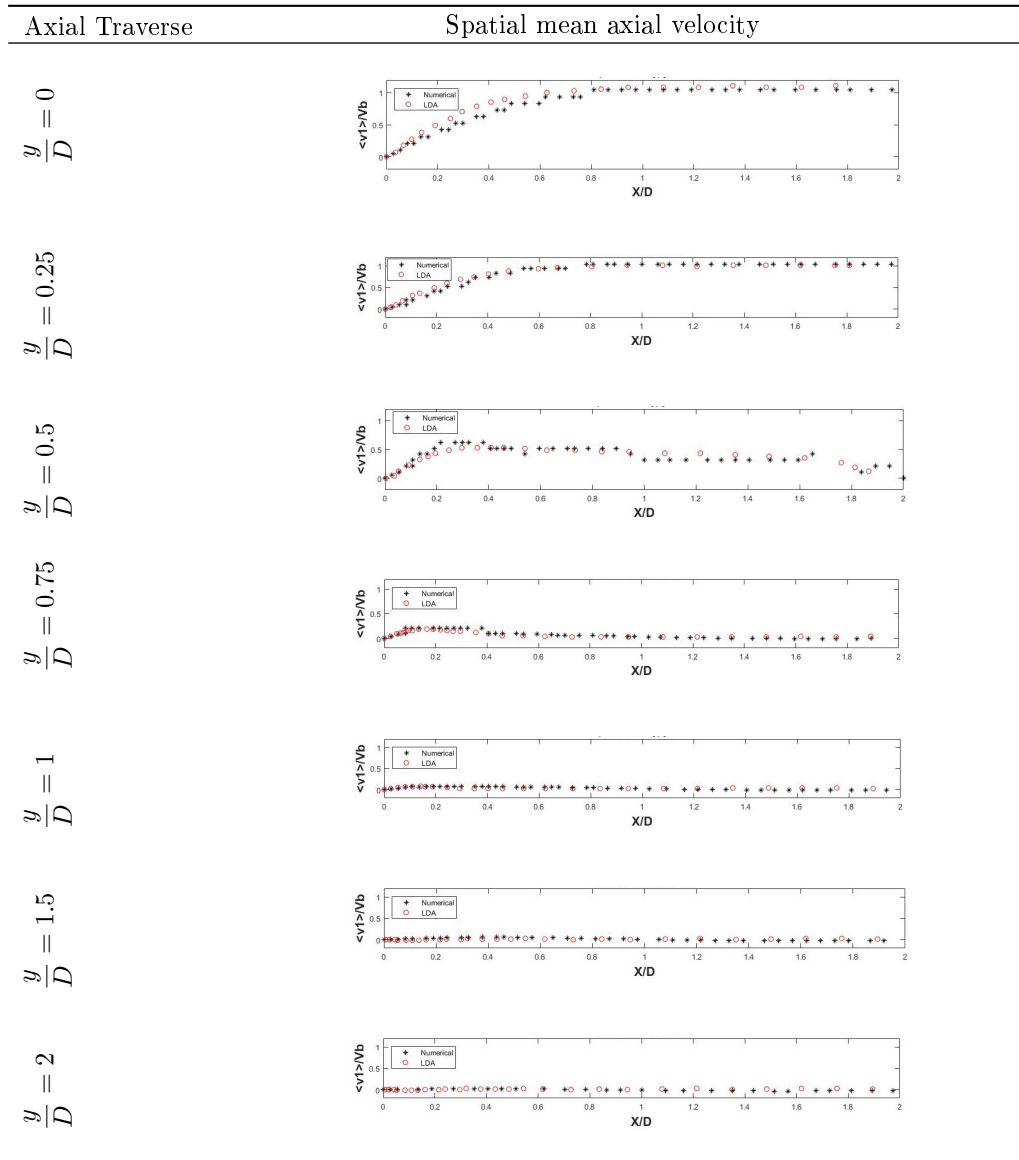


Table 1: Mean Axial velocity component at different axial traverses, LDA data from Mark J. Tummers et al [6].

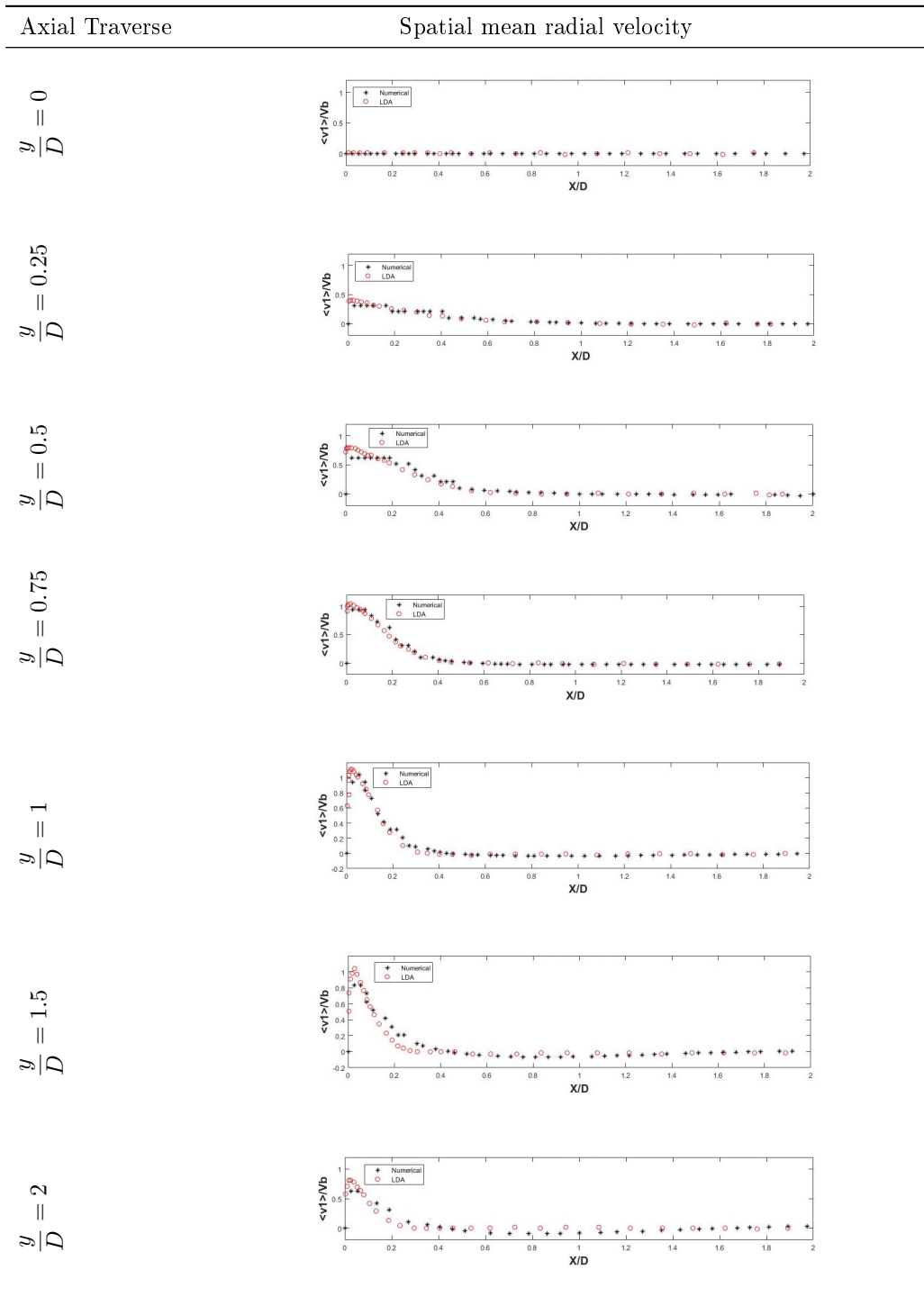


Table 2: Mean Radial velocity component at different axial traverses, LDA data from Mark J. Tummers et al [6].

3.2 Eye FSI coupled model

Figure 6 shows the fully coupled FSI model of the air jet CFD model and the FE model of the eye. All the information such as the pressure distribution on the cornea, the air velocity, the stresses and deformation of the cornea can be extracted at real time and direct response to the effect of the air puff which gives a

great advantage of data analysis, parametric studies and material characterisation. By using Python code, the information can be extracted from Abaqus output database files and then analysed by Matlab to do the comparison with clinical data.

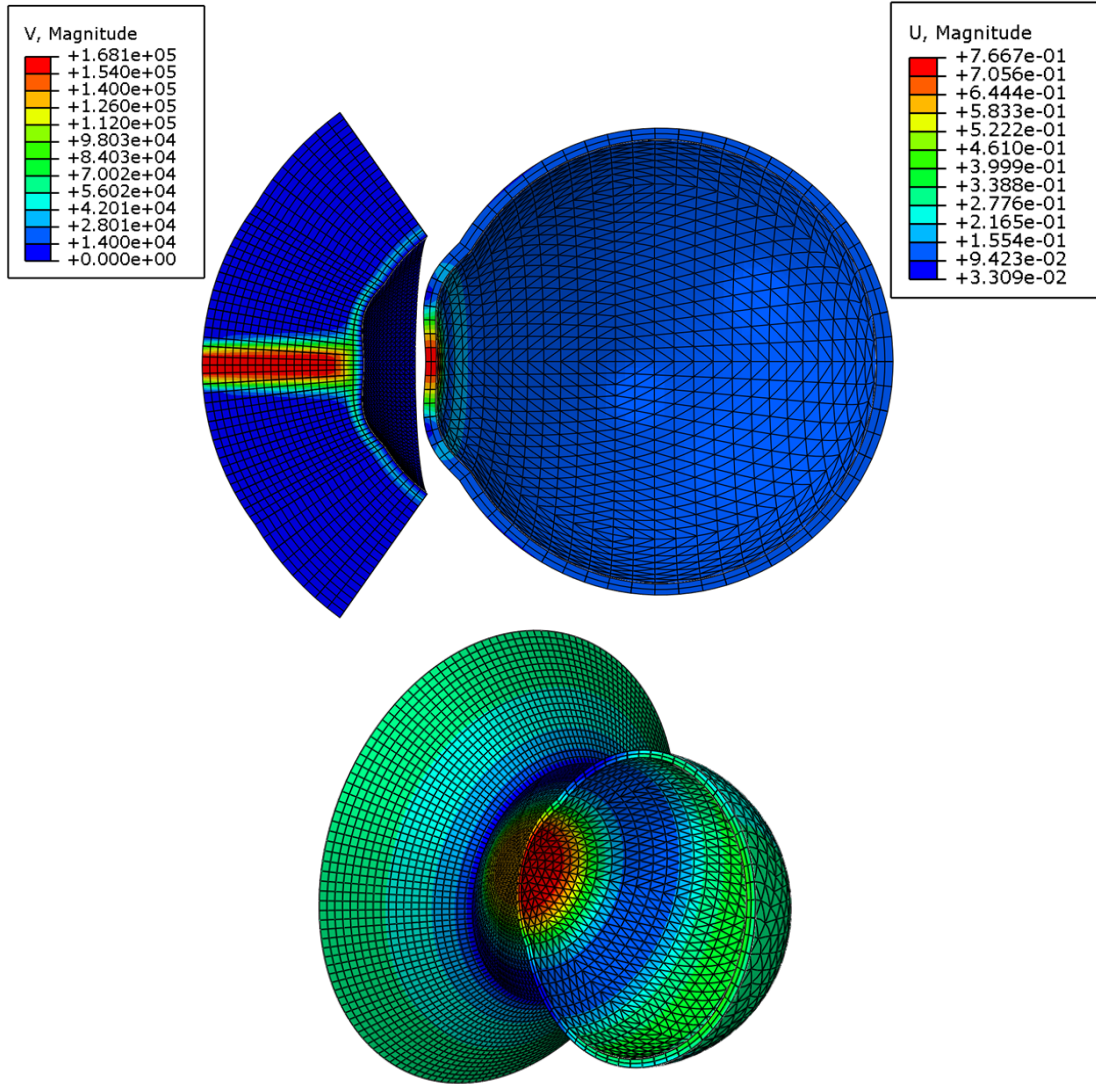


Figure 6: The FSI coupled model of the eye showing the velocity magnitude of the air jet and the eye model deformation magnitude.

3.3 Pressure and deformation profiles

Fluid structure interaction has an effect on the pressure distribution on the cornea during the time of the air puff test. Table 3 shows the pressure distribution on the cornea at different time steps during the test and it showed complete different behaviour than what was assumed in the literature and previous simulations of the air puff test. Graph (a) shows the exact pressure distribution and the region where there is negative pressure. Graph (b) shows the progression of the cornea deformation with time. To show the effect of the cornea flexibility on the pressure values of the jet, two different simulations of the turbulent jet have been performed on a rigid cornea shape surface with no moving boundaries. One model for the cornea at the initial shape and the other model is at the maximum deformation geometry, but the cornea surface is solid with no slip wall boundary condition. When the results of these two models have been compared with the

FSI model considering flexible cornea, it illustrates the difference clearly as shown in figure 8.

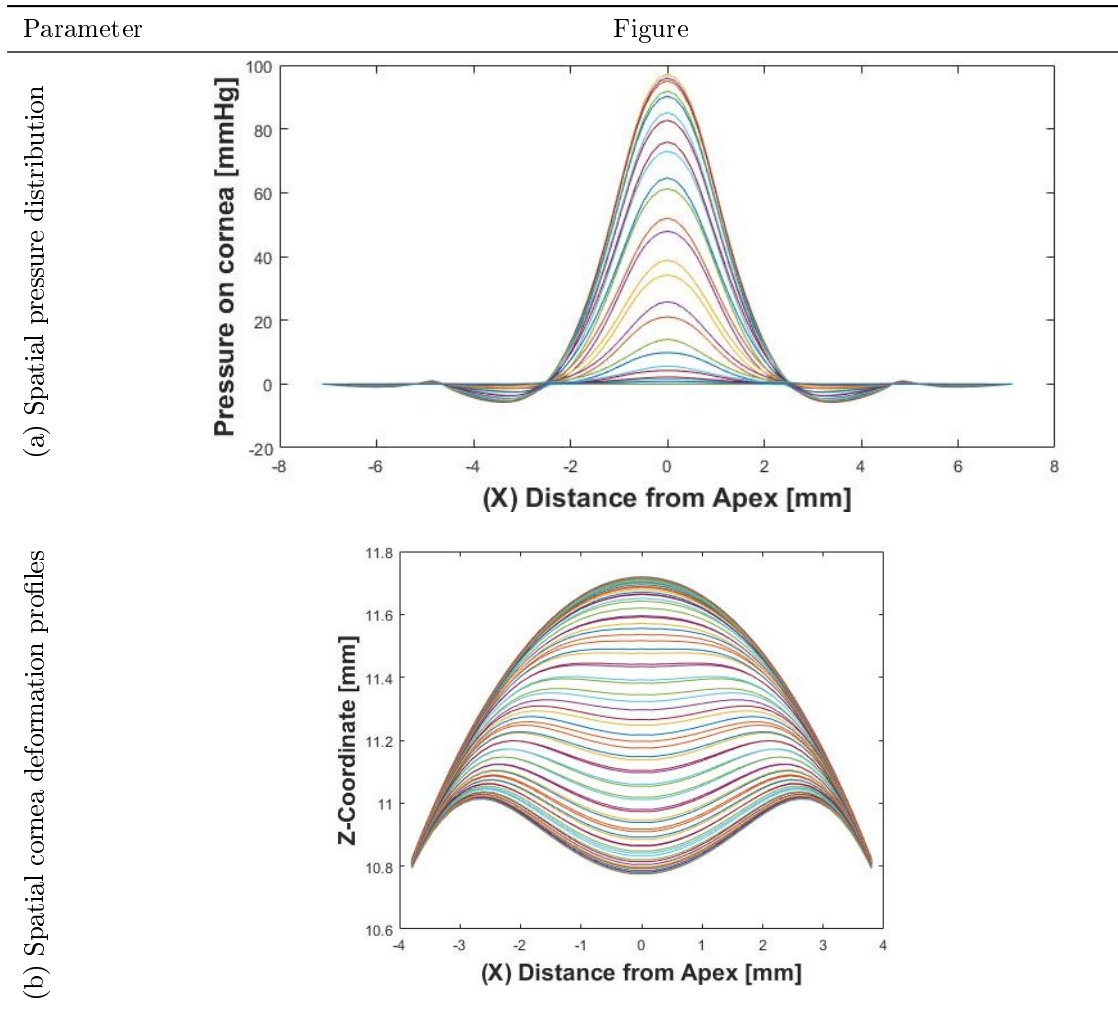


Table 3: Pressure distribution on the cornea at every 1 ms of the test (a), and deformation of the cornea at every 0.1 ms of the test

3.4 Comparison with clinical data from CorVis-ST

Figure 7 (a) shows the cornea deformation profiles comparison numerically and clinically on real patients. The maximum deformation for the clinical case is 0.9 mm and for the numerical model is 0.81 mm with percentage error of 10%. The thickness of the cornea (CCT), the IOP and the age affect the response of the cornea to the air puff pressure. The age affects the cornea material stiffness as it get stiffer with elder ages. Figure ?? (b) shows the cornea apex deformation with time during the test. The hysteresis effect is clear between the numerical and the clinical response of the cornea and ths one of the important recommendations from the FSI model to improve the material model. The other significant source of error is the rebounding of the whole eye due to the impact of the air puff as the eye is surrounded by a flexible fatty tissue that allow the eye to move backward.

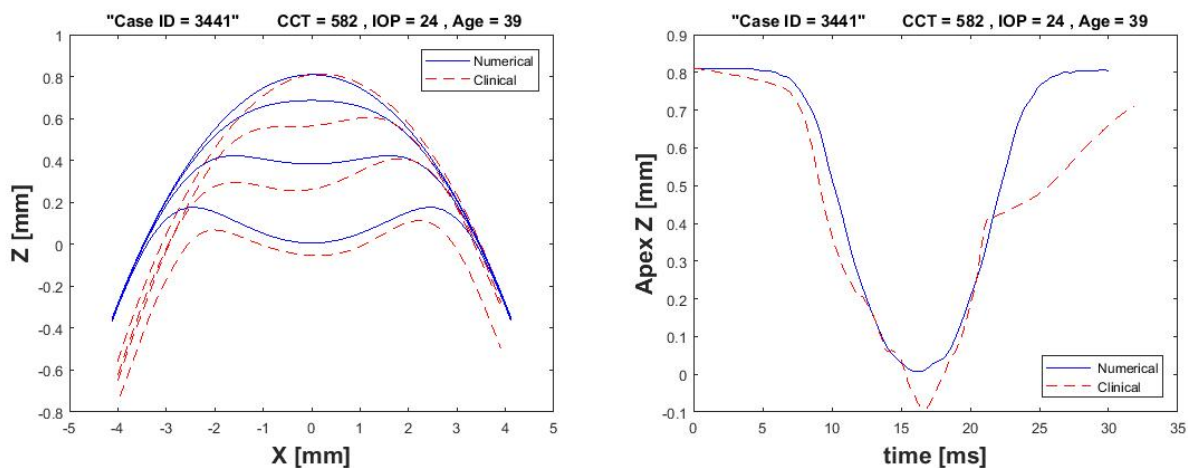


Figure 7: The deformation profiles of the cornea during the air puff test every 0.1 ms (a) and the apex deformation with time (b).

Figure 8 illustrates the difference in the pressure distribution on the cornea for two numerical models one with FSI and the other without the FSI simulation. Also, the deformation profiles of the cornea has been compared numerically and clinically with applying two different turbulence models for the air puff, Spallart Allmaras and RNG $K-\epsilon$ (Renormalisation Group) and been found that there is no change in the results.

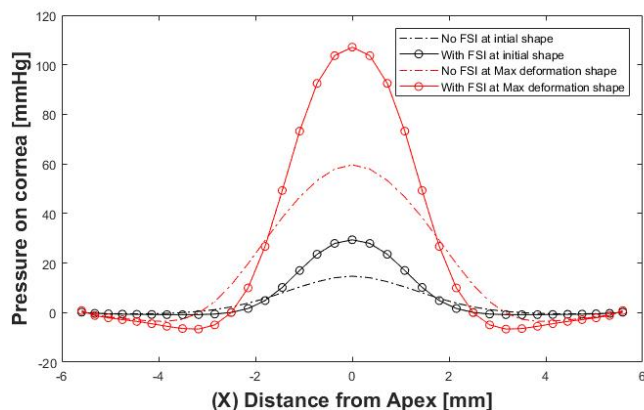


Figure 8: Pressure distribution comparison on the cornea with and without FSI effect.

4 Discussion

The air puff test is a non contact method to measure the eye internal pressure noninvasively, but compared to the gold standard of IOP contact measurement techniques, it's been found influenced by the biomechanical properties of the eye, either the geometry parameters like cornea thickness or radius, or the material properties which has been reported to change from person to another and with age variation as well. So the main question is how we can make this technique valid for everyone having the eye test with the minimum amount of error. The answer to this question is the primary argument of the current study. The biomechanical correction of the IOP measurement has been the focus of many studies in the past.

Some studies focused on the association of the IOP with the cornea CCT and Radius, other studies

studied the material properties effect, but most of the them were structural in nature with no sufficient attention to the fluid structure interaction effect during the air puff test, especially due to the fact that the corneal tissue is bounded by two fluids, the air jet from outside and the aqueous and vitreous humour from inside. This is considered a significant fluid mechanics analysis which can't be simplified or perform the structural and material analysis based on assumptions on the fluid interaction with the material. Some of these assumptions can work effectively if the ratio between the time scales of the two physics is very small or very large to neglect the effect of one domain over the other or make a reasonable approximation, this ratio is known as the reduced velocity (U_R). But this is not the case in the air puff test as the two time scales of the fluid velocity and the eye deformations are within the same order of magnitude and changing through the unsteady application of the air jet on the cornea during the test. That's the core of any fluid structure interaction problem classification as there are plenty of applications and numerical methods specific to each kind of problem.

The numerical analysis of the turbulent impinging jet has been done in the context of hybrid finite volume solution of Navier-Stokes equations and Spallart allmaras or RNG k- ϵ turbulence models to simulate the production and dissipation of the turbulent kinetic energy which will produce an approximate solution for the pressure and the velocity fields over the cornea surface. The produced solution for the pressure distribution on the cornea and its progression with time is a significant improvement in the understanding of the change of the pressure with time during the test compared to what have been assumed in the literature.

The numerical analysis of the finite element model of the eye has been done based on the context of the previous research conducted at the Biomechanics group. It uses the Galerkin mean weighted residual method to calculate the global stiffness matrix and then calculate the deformation of the nodes. The approximation on the air puff pressure was based on a constant pressure loading at the different rings of the cornea changing in magnitude during the time of the test. This pressure distribution is provided by Oculus based on the pressure transducer reading inside the cylinder and the pressure on the cornea is been approximated to be half of the piston pressure [7].

Regarding the difference between the numerical spatial deformation profiles of the cornea compared to the clinical measurement, there is a difference due to the fact that the existing material model of the eye has some approximations and doesn't match exactly with the clinical behaviour which is a hard target to achieve as the material properties affected by a lot of biomechanical parameters and from person to another. The boundary conditions also fix the eye from moving in the anterior posterior direction which is not the case in the real eye which is allowed to bounce back in response to the air puff impact. The other effect is the hysteresis effect of the cornea after removing the load, the real cornea has some memory effect and takes time to return back to the original geometry. This effect is not considered in the numerical model of the eye which is a good achievement of the current study.

5 Conclusion and Future Work

The complete coupling between the model of the eye and the air model has been accomplished also mesh independence test, boundary conditions independence test. The main finding is that the pressure distribution of the air puff is changing with the time of the test. A parametric study has been done to see the effect of the corneal biomechanical parameters on the IOP measurements and come up with a biomechanically corrected equation. The next required work is to compare these numerical results with more experimental data from human and porcine eyes. Once we validate this model, this will open the doors for inverse analysis to get the right material properties of the cornea or to consider the corneal hysteresis and gain better understanding of the cornea behaviour under loading by testing diseased cornea such as corneal ectasia or corneas after and before cross linking. Also, the simulation of the orbit and the fatty tissue around the eye is recommended to reach with the eye model to a higher level of accuracy.

References

- [1] Harry A. Quigley. Glaucoma. *Lancet*, 377:1367–1377, 2011.
- [2] Ahmed Elsheikh, Defu Wang, Achal Kotecha, Michael Brown, and David Garway-Heath. Evaluation of

- Goldmann applanation tonometry using a nonlinear finite element ocular model. *Annals of Biomedical Engineering*, 34(10):1628–40, oct 2006.
- [3] JW Gauntner, John N B Livingood, and P Hrycak. Survey of literature on flow characteristics of a single turbulent jet impinging on a flat plate. *Washington, DC*, (February):43, 1970.
 - [4] Coleman Dup D and D S Snedeker. A study of free jet impingement. Part 1. Mean properties of free and impinging jets. *Journal of Fluid Mechanics*, 45(2):281–319, 1971.
 - [5] Khaled J. Hammad and Ivana Milanovic. Flow Structure in the Near-Wall Region of a Submerged Impinging Jet. *Journal of Fluids Engineering*, 133(9):091205, 2011.
 - [6] Mark J. Tummers, Jeroen Jacobse, and Sebastiaan G J Voorbrood. Turbulent flow in the near field of a round impinging jet. *International Journal of Heat and Mass Transfer*, 54(23-24):4939–4948, 2011.
 - [7] Akram Abdelazim Joda, Mir Mohi Sefat Shervin, Daniel Kook, and Ahmed Elsheikh. Development and validation of a correction equation for corvis tonometry. *Computer Methods in Biomechanics and Biomedical Engineering*, 19(9):943–953, 2016. PMID: 27049961.
 - [8] N. Rajaratnam, D. Z. Zhu, and S. P. Rai. Turbulence measurements in the impinging region of a circular jet. *Canadian Journal of Civil Engineering*, 37(2002):782–786, 2010.
 - [9] D. Cooper, D. C. Jackson, B. E. Launder, and G. X. Liao. Impinging jet studies for turbulence model assessment-I. Flow-field experiments. *International Journal of Heat and Mass Transfer*, 36(10):2675–2684, 1993.
 - [10] Hussein J. Hussein, Steven P. Capp, and William K. George. Velocity measurements in a high-Reynolds-number, momentum-conserving, axisymmetric, turbulent jet. *Journal of Fluid Mechanics*, 258(1994):31–75, 1994.
 - [11] Ahmed Elsheikh, Defu Wang, and David Pye. Determination of the modulus of elasticity of the human cornea. *Journal of refractive surgery (Thorofare, N.J. : 1995)*, 23(8):808–18, oct 2007.
 - [12] Aachal Kotecha, Ahmed Elsheikh, Cynthia R Roberts, Haogang Zhu, and David F Garway-Heath. Corneal thickness- and age-related biomechanical properties of the cornea measured with the ocular response analyzer. *Investigative ophthalmology & visual science*, 47(12):5337–47, dec 2006.
 - [13] P G Davey, a Elsheikh, and D F Garway-Heath. Clinical evaluation of multiparameter correction equations for Goldmann applanation tonometry. *Eye (London, England)*, (January):1–9, mar 2013.
 - [14] Ahmed Elsheikh, Pinakin Guntant, Stephen W Jones, David Pye, and David Garway-Heath. Correction factors for Goldmann Tonometry. *Journal of glaucoma*, 22(2):156–63, feb 2013.
 - [15] Ahmed Elsheikh, Daad Alhasso, Aachal Kotecha, and David Garway-Heath. Assessment of the ocular response analyzer as a tool for intraocular pressure measurement. *Journal of biomechanical engineering*, 131(8):081010, aug 2009.
 - [16] Craig Boote, Joel R Palko, Thomas Sorensen, Ashkan Mohammadvali, Ahmed Elsheikh, and M Andrés. Changes in posterior scleral collagen microstructure in canine eyes with an ADAMTS10 mutation. 10(November 2015):503–517, 2016.
 - [17] Mohammad Arsalan Khan. Numerical study on human cornea and modified multiparametric correction equation for Goldmann applanation tonometer. *Journal of the mechanical behavior of biomedical materials*, 30:91–102, feb 2014.
 - [18] Michael Sullivan-Mee, Sarah E Lewis, Denise Pensyl, Gretchen Gerhardt, Kathy D Halverson, and Clifford Qualls. Factors Influencing Intermethod Agreement Between Goldmann Applanation, Pascal Dynamic Contour, and Ocular Response Analyzer Tonometry. *Journal of glaucoma*, 00(00):1–9, mar 2012.
 - [19] Original Article. EVALUATING THE MATERIAL PARAMETERS OF THE HUMAN r Fo Pe er Re vi ew Fo r P ee r R. 2009.
 - [20] Andrew S H Tsai and Seng Chee Loon. Intraocular pressure assessment after laser in situ keratomileusis: a review. *Clinical & experimental ophthalmology*, 40(3):295–304, apr 2012.
 - [21] Javier Moreno-Montañés, Miguel J Maldonado, Noelia García, Loreto Mendiluce, Pio J García-Gómez, and María Seguí-Gómez. Reproducibility and clinical relevance of the ocular response analyzer in nonoperated eyes: corneal biomechanical and tonometric implications. *Investigative ophthalmology & visual science*, 49(3):968–74, mar 2008.
 - [22] H Studer, X Larrea, H Riedwyl, and P Büchler. Biomechanical model of human cornea based on stromal microstructure. *Journal of biomechanics*, 43(5):836–42, mar 2010.
 - [23] Visual Science, Wai Lun, Ka Kit, and Visual Sciences. r Fo ew On r Fo Re ew On ly. 2011.

- [24] FangJun Bao, ManLi Deng, QinMei Wang, JinHai Huang, Jing Yang, Charles Whitford, Brendan Geraghty, AYong Yu, and Ahmed Elsheikh. Evaluation of the relationship of corneal biomechanical metrics with physical intraocular pressure and central corneal thickness in ex vivo rabbit eye globes. *Experimental Eye Research*, 137(August):11–17, 2015.
- [25] K Anderson, a El-Sheikh, and T Newson. Application of structural analysis to the mechanical behaviour of the cornea. *Journal of the Royal Society, Interface / the Royal Society*, 1(1):3–15, nov 2004.
- [26] Etsuo Chihara. Assessment of true intraocular pressure: the gap between theory and practical data. *Survey of ophthalmology*, 53(3):203–18, 2008.
- [27] Ahmed Elsheikh, Brendan Geraghty, Daad Alhasso, Jonathan Knappett, Marino Campanelli, and Paolo Rama. Regional variation in the biomechanical properties of the human sclera. *Experimental Eye Research*, 90(5):624–33, may 2010.
- [28] Rafael Grytz, Massimo A Fazio, Vincent Libertiaux, Luigi Bruno, Stuart Gardiner, Christopher A Girkin, and J Crawford Downs. Age- and Race-Related Differences in Human Scleral Material Properties. 2014.
- [29] Kristin M Myers, Frances E Cone, Harry A Quigley, Scott Gelman, and Mary E Pease. NIH Public Access. 91(6):866–875, 2011.
- [30] Sabine Kling, Nandor Bekesi, Carlos Dorronsoro, Daniel Pascual, and Susana Marcos. Corneal Viscoelastic Properties from Finite-Element Analysis of In Vivo Air-Puff Deformation. 9(8), 2014.
- [31] Alfonso Pé, Jos Requejo, Requejo Isidro, and Susana Marcos. Corneal Deformation in an Inflation Porcine Corneal Model Measured with Scheimpflug Imaging Conclusions. 2008.
- [32] Xiaoyu Liu, Lizhen Wang, Jing Ji, Wei Yao, Wei Wei, Jie Fan, Shailesh Joshi, Deyu Li, and Yubo Fan. A Mechanical Model of the Cornea Considering the Crimping Morphology of Collagen Fibrils. 2013.
- [33] David P. Piñero and Natividad Alcón. In vivo characterization of corneal biomechanics. *Journal of Cataract and Refractive Surgery*, 40(6):870–887, 2014.
- [34] Christopher Kai-Shun Leung, Cong Ye, and Robert N Weinreb. An ultra-high-speed Scheimpflug camera for evaluation of corneal deformation response and its impact on IOP measurement. *Investigative ophthalmology & visual science*, 54(4):2885–92, apr 2013.
- [35] Aachal Kotecha, David P Crabb, Alexander Spratt, and David F Garway-Heath. The relationship between diurnal variations in intraocular pressure measurements and central corneal thickness and corneal hysteresis. *Investigative ophthalmology & visual science*, 50(9):4229–36, sep 2009.
- [36] Chuanqing Zhou Zhaolong, Han, Dai, Zhou. Air Puff Induced Corneal Vibrations : Theoretical. (August 2015), 2014.
- [37] Meixiao Shen, Jianhua Wang, Jia Qu, Suzhong Xu, Xiaoxing Wang, Haizhen Fang, and Fan Lu. Diurnal variation of ocular hysteresis, corneal thickness, and intraocular pressure. *Optometry and vision science : official publication of the American Academy of Optometry*, 85(12):1185–92, dec 2008.
- [38] Ian a Sigal. An applet to estimate the IOP-induced stress and strain within the optic nerve head. *Investigative ophthalmology & visual science*, 52(8):5497–506, jul 2011.
- [39] Kristin M Myers, Baptiste Coudrillier, Brad L Boyce, and Thao D Nguyen. The inflation response of the posterior bovine sclera. *Acta biomaterialia*, 6(11):4327–35, nov 2010.
- [40] Ian a Sigal, Richard a Bilonick, Larry Kagemann, Gadi Wollstein, Hiroshi Ishikawa, Joel S Schuman, and Jonathan L Grimm. The optic nerve head as a robust biomechanical system. *Investigative ophthalmology & visual science*, 53(6):2658–67, may 2012.
- [41] Ahmed Elsheikh and Defu Wang. Numerical modelling of corneal biomechanical behaviour. *Computer methods in biomechanics and biomedical engineering*, 10(2):85–95, apr 2007.
- [42] Keith M Meek and Craig Boote. The use of X-ray scattering techniques to quantify the orientation and distribution of collagen in the corneal stroma. *Progress in retinal and eye research*, 28(5):369–92, sep 2009.
- [43] Shang Wang, Jiasong Li, Ravi Kiran Manapuram, Floredes M Menodiado, R Davis, Michael D Twa, Alexander J Lazar, Dina C Lev, and Raphael E Pollock. HHS Public Access. 37(24):5184–5186, 2015.
- [44] David R Lari, David S Schultz, Aaron S Wang, On-Tat Lee, and Jay M Stewart. Scleral mechanics: comparing whole globe inflation and uniaxial testing. *Experimental eye research*, 94(1):128–35, jan 2012.
- [45] Meixiao Shen, Fan Fan, Anquan Xue, Jianhua Wang, Xiangtian Zhou, and Fan Lu. Biomechanical properties of the cornea in high myopia. *Vision research*, 48(21):2167–71, sep 2008.
- [46] Ahmed Elsheikh, Defu Wang, Michael Brown, Paolo Rama, Marino Campanelli, and David Pye. As-

- assessment of corneal biomechanical properties and their variation with age. *Current Eye Research*, 32(1):11–19, jan 2007.
- [47] Andrew Lam, Davie Chen, Roger Chiu, and Wan-Sang Chui. Comparison of IOP measurements between ORA and GAT in normal Chinese. *Optometry and vision science : official publication of the American Academy of Optometry*, 84(9):909–14, sep 2007.
- [48] Ahmed Elsheikh, Wael Kassem, and Stephen W Jones. Strain-rate sensitivity of porcine and ovine corneas. *Acta of bioengineering and biomechanics / Wrocław University of Technology*, 13(2):25–36, jan 2011.
- [49] Kirsten E Hamilton and David C Pye. Young’s modulus in normal corneas and the effect on applanation tonometry. *Optometry and vision science : official publication of the American Academy of Optometry*, 85(6):445–50, jun 2008.
- [50] S Salimi, S Simon Park, and T Freiheit. Dynamic Response of Intraocular Pressure and Biomechanical Effects of the Eye Considering Fluid-Structure Interaction. 133(September 2011):1–11, 2015.
- [51] Kimberly M. Metzler, Ashraf M. Mahmoud, Jun Liu, and Cynthia J. Roberts. Deformation response of paired donor corneas to an air puff: Intact whole globe versus mounted corneoscleral rim. *Journal of Cataract and Refractive Surgery*, 40(6):888–896, 2014.
- [52] Adrian Smedowski, Beata Weglarz, Dorota Tarnawska, Kai Kaarniranta, and Edward Wylegala. Comparison of three intraocular pressure measurement methods including biomechanical properties of the cornea. *Investigative ophthalmology & visual science*, 55(2):666–73, feb 2014.
- [53] Aurélie Benoit, Gaël Latour, Schanne-Klein Marie-Claire, and Jean-Marc Allain. Simultaneous microstructural and mechanical characterization of human corneas at increasing pressure. *Journal of the Mechanical Behavior of Biomedical Materials*, 60:93–105, 2016.
- [54] Ahmed Elsheikh, Charles W. McMonnies, Charles Whitford, and Gavin C. Boneham. In vivo study of corneal responses to increased intraocular pressure loading. *Eye and Vision*, 2(1):20, 2015.
- [55] Kristin M Myers, Frances E Cone, Harry a Quigley, Scott Gelman, Mary E Pease, and Thao D Nguyen. The in vitro inflation response of mouse sclera. *Experimental eye research*, 91(6):866–75, dec 2010.
- [56] David Touboul, Cynthia Roberts, Julien Kérautret, Caroline Garra, Sylvie Maurice-Tison, Elodie Saubusse, and Joseph Colin. Correlations between corneal hysteresis, intraocular pressure, and corneal central pachymetry. *Journal of cataract and refractive surgery*, 34(4):616–22, apr 2008.
- [57] Abhijit Sinha Roy and William J Dupps. Patient-specific modeling of corneal refractive surgery outcomes and inverse estimation of elastic property changes. *Journal of biomechanical engineering*, 133(1):011002, jan 2011.
- [58] Charles W McMonnies. Assessing corneal hysteresis using the Ocular Response Analyzer. *Optometry and vision science : official publication of the American Academy of Optometry*, 89(3):E343–9, mar 2012.
- [59] Benjamin Cruz Perez, Hugh J Morris, Richard T Hart, and Jun Liu. Finite element modeling of the viscoelastic responses of the eye during microvolumetric changes. *Journal of biomedical science and engineering*, 6(12A):29–37, dec 2013.
- [60] Ahmed Elsheikh, Defu Wang, Paolo Rama, Marino Campanelli, and David Garway-Heath. Experimental assessment of human corneal hysteresis. *Current Eye Research*, 33(3):205–13, mar 2008.
- [61] Bodies Mechanics and Biomedical Sciences. r Fo vi ew On Fo r R iew On ly. 2009.
- [62] David Pye, Vision Science, and Ocular Response Analyser. Title page. 3424:1–26, 2011.
- [63] Visual Science. r Fo ew On r Fo Re ew On ly. 2010.
- [64] Ying Hon and Andrew K C Lam. Corneal deformation measurement using Scheimpflug noncontact tonometry. *Optometry and vision science : official publication of the American Academy of Optometry*, 90(1):e1–8, jan 2013.
- [65] Steven J Petsche and Peter M Pinsky. The role of 3-D collagen organization in stromal elasticity: a model based on X-ray diffraction data and second harmonic-generated images. *Biomechanics and modeling in mechanobiology*, (1938), jan 2013.
- [66] Ian C Campbell. Biomechanics of the Posterior Eye : A Critical Role in Health and Disease. 136(February 2014), 2016.
- [67] K M Meek. The Cornea and Sclera. 2008.
- [68] Jun Liu and Xiaoyin He. Corneal stiffness affects IOP elevation during rapid volume change in the eye. *Investigative ophthalmology & visual science*, 50(5):2224–9, may 2009.